Energy saving potential of night ventilation:
Sensitivity to pressure coefficients for different European climates

R. Ramponi [(a,b)], A. Angelotti [(c)] ∗, B. Blocken [(b,d)]
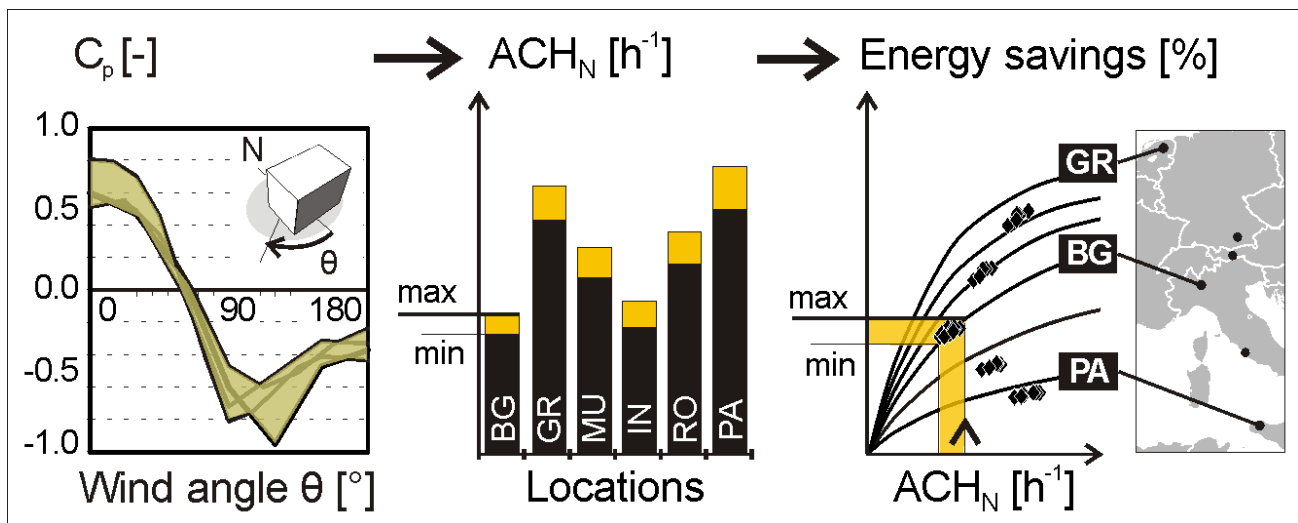
(a) Architecture, Built Environment, Construction Engineering Department, Politecnico di Milano, via Ponzio 31, 20133 Milano, Italy
(b) Building Physics and Services, Eindhoven University of Technology, P.O. box 513, 5600 MB Eindhoven, the Netherlands
(c) Energy Department, Politecnico di Milano, via Lambruschini 4, 20156 Milano, Italy
(d) Building Physics Section, Department of Civil Engineering, Kasteelpark Arenberg 40 – bus 2447, 3001 Heverlee, Belgium

Graphical abstract

∗ **Corresponding author**: Adriana Angelotti, Energy Department, Politecnico di Milano, v. Lambruschini 4, 20133 Milano, Italy. Tel.: +39 02 2399 5183, Fax +39 02 2399 3913*;E-mail address:* adriana.angelotti@polimi.it

Energy saving potential of night ventilation:
Sensitivity to pressure coefficients for different European climates

R. Ramponi [(a,b)], A. Angelotti [(c)] *, B. Blocken [(b,d)]

(a) Architecture, Built Environment, Construction Engineering Department, Politecnico di Milano, via Ponzio 31, 20133 Milano, Italy
(b) Building Physics and Services, Eindhoven University of Technology, P.O. box 513, 5600 MB Eindhoven, the Netherlands
(c) Energy Department, Politecnico di Milano, via Lambruschini 4, 20156 Milano, Italy
(d) Building Physics Section, Department of Civil Engineering, Kasteelpark Arenberg 40 – bus 2447, 3001 Heverlee, Belgium

Abstract

The suitability of night ventilation to reduce the cooling demand in buildings can be evaluated by coupling Airflow Network Models to Building Energy Simulation tools. To estimate wind-induced ventilation, pressure coefficients (C_p) on the building envelope are key inputs, as well as local wind speed and direction. C_p data obtained by primary sources such as measurements or CFD simulations are considered the most reliable but can be difficult to obtain. An easy alternative are C_p secondary sources, such as databases providing literature data correlations. Therefore an issue arises regarding the choice of the source of pressure coefficients.

This paper investigates the effects of C_p from primary and secondary sources on the predicted energy saving potential of night ventilation of an isolated office building for several European climates and some relevant design conditions and simulation parameters. Different C_p sources produce a dispersion of C_p data and differences in the calculated night ventilation rates up to 15%. Contrary to what might be expected, these differences influence only marginally the resulting passive cooling effects. Overall a stronger impact is observed for the colder climates, where higher temperature differences occur between desired indoor temperature and night-averaged outdoor temperature. Finally, for the building under study, the choice of the C_p source appears less crucial than the choice of other building simulation parameters, such as the internal convective heat transfer coefficient. This study can support building designers towards accurate energy simulations of naturally ventilated buildings.

Keywords: Ventilation; Cooling; Pressure Coefficient; Airflow Network; Energy; Simulation.

1. Introduction

According to the European Directive for the energy performance of buildings [1] the building sector accounted in 2002 for almost the 40% of the European energy consumption. Among end uses in buildings, summer air conditioning is growing, leading to an increase in overall and peak electricity consumption. Due to climate change, outdoor air temperature is expected to rise substantially, suggesting an increasing importance of advanced passive cooling measures to limit the summer energy demand [2].

Night cooling, meant as the combined effect of both natural or mechanical night ventilation, and building thermal inertia, was proven to be an effective measure to reduce cooling loads [3-5]. The heat absorbed by the building exposed thermal mass during the day is released to the indoor air at night, after which it is purged by night ventilation. Meanwhile, external fresh air cools down the thermal mass which then acts as a heat sink in the following day [4]. The efficiency of night cooling depends on the thermal properties of the building and on the local climate conditions, i.e. night-time wind speed and temperature swing of the ambient air [3,6-8]. A Climatic Cooling Potential (CCP) index based on the indoor-outdoor night temperature difference was established by Artmann et al. [9] to map the regions with sufficient night cooling potential.

In order to calculate cooling energy savings in buildings with natural ventilation, an airflow analysis has to be coupled with a thermal model as used by Building Energy Simulation tools. Accurate airflow analyses can be performed with experiments or Computational Fluid Dynamics [10-16] . However, issues related with the complexity of the models, the required time and expertise and the possibility of integration with the energy simulation tools arise. A good trade-off was found in the so-called 'Airflow Network (AFN) Models', which are suited for integration with Building Energy Simulation tools [17,18]. AFN models are based on the mass balance within several zonal nodes connected by airflow elements, e.g. openings, doors, or cracks [19]. Each zonal node is characterized by temperature and pressure conditions, while correlations between pressure difference and airflow are assigned to the airflow elements. Boundary conditions for natural ventilation are imposed at the external nodes to express the wind pressure on the envelope by means of

---
* **Corresponding author**: Adriana Angelotti, Energy Department, Politecnico di Milano, v. Lambruschini 4, 20133 Milano, Italy. Tel.: +39 02 2399 5183, Fax +39 02 2399 3913; *E-mail address:* adriana.angelotti@polimi.it

pressure coefficients (C_p). Pressure coefficients relate the static pressure at a given point of the building facade (P_x) to the reference static (P_{ref}) and dynamic (P_{dyn}) pressure as in Eq.1, where P_{dyn} depends on air density (ρ) and reference wind speed (U_{ref}). Usually, U_{ref} and P_{ref} are taken at building height in the upstream undisturbed flow.

$$C_P = \frac{P_x - P_{ref}}{P_{dyn}} = \frac{P_x - P_{ref}}{0.5 \cdot \rho \cdot U_{ref}^2} \qquad (1)$$

C_p values are strongly related to building geometry and facade design, and to the local wind conditions e.g. wind incident profile, or presence of surrounding obstacles. Therefore AFN models usually allow user-defined sets of C_p obtained from external 'primary sources', i.e. measurements or numerical simulations, or from 'secondary sources', i.e. databases or analytical models [20,21]. Primary sources are considered the most reliable for airflow calculations, albeit less accessible. Secondary sources are therefore most often used in practice, increasing the uncertainty of the predicted wind-driven airflow rates [20]. The use of surface-averaged C_p in spite of local values at the right flow path location increases the uncertainties of the calculations [20,22]. Past studies [23] reported differences between 5% and 10% in the ventilation rates estimated using the local or the surface-averaged C_p.

The performance of night ventilation in buildings has been often evaluated in terms of indoor thermal comfort under free-floating conditions. In particular, many studies in the past focused on the impact of the local climate [6,9,24] and other design conditions, e.g. building thermal mass [25,26] or internal heat gains [24,27,28]. However, the accuracy of the calculation is also affected by simulation parameters like the internal Convective Heat Transfer Coefficients (CHTC), the discharge coefficient of the openings (C_D) or the wind pressure coefficients C_p [27,29]. Focusing on daytime thermal comfort, Breesch and Janssens [29] presented a comprehensive analysis of the most influential input parameters for the evaluation of night ventilation performance. A sensitivity analysis based on Standardized Regression Coefficients was performed. Among others, the deviation of the wind pressure coefficients due to the uncertainty in the wind shielding conditions of the building is also considered. The wind pressure coefficients resulted to be a relevant parameter for natural night ventilation. However, a higher impact was associated to the internal heat gains, the air tightness, the solar heat gain coefficient of sun blinds and the internal Convective Heat Transfer Coefficient. To the best of the authors' knowledge the sensitivity to the dispersion of the C_p values due to different primary and secondary sources has not been clarified yet. Moreover, the effectiveness of night ventilation is rarely evaluated in terms of cooling energy savings rather than comfort conditions. Nevertheless, night ventilation in combination with an active cooling device is often used in office buildings and in warm climates and the related cooling energy savings are therefore relevant to consider.

Therefore in this paper, the influence of primary and secondary C_p sources on the summer energy savings of an isolated night-ventilated building is investigated and discussed. The influence of the local climate and other design conditions and simulation parameters on the sensitivity to the C_p sources is further explored. A six-story office building is adopted as case study and modeled in EnergyPlus [30]. C_p values calculated with EnergyPlus using the formula of Swami and Chandra [31] are compared with others obtained with (i) the web-based software CpGenerator [32], (ii) the program CPCALC+ [33], and (iii) the wind tunnel tests by Tokyo Polytechnic University (TPU) [34,35] (Sect. 4.1).

At first, the influence of night ventilation rates on the cooling energy savings is investigated by means of a sensitivity analysis conducted under constant ventilation rates for different locations (Sect. 4.2). Then, the AFN model in EnergyPlus is used to analyze the impact of the C_p sources on the predicted night ventilation rates and the relative cooling energy savings for each location (Sect. 4.3 and 4.5). A detailed analysis is carried out for the location of Bergamo that is characterized by high night ventilation potential and building cooling demand (Sect. 4.3). In Bergamo the impact on the sensitivity to the C_p source of other relevant parameters in the evaluation of the natural night ventilation, as identified e.g. by [6, 9, 24-29], is analyzed (Sect. 4.4). In particular it has been considered the variation of design conditions, i.e. thermal inertia of the exposed thermal mass, internal heat gains and set point temperature, and the variation of simulation parameters, i.e. interior Convective Heat Transfer Coefficients and discharge coefficient of the openings. Finally, the results obtained with the sensitivity analysis for different European climates and with the AFN model are compared and discussed (Sect. 4.5), and some limitations of the study are pointed out (Sect. 4.6).

Nomenclature

A	Surface-averaged
ACH	Air Changes per Hour (h^{-1})
AFN	Air Flow Network
AIJ	Architectural institute of Japan
ALS	Alpine south
ATN	Atlantic north
BG	Bergamo
C_D	Discharge coefficient
C_p	Pressure coefficient
CHTC	Convective heat transfer coefficient (W/(m²K))

CON	Continental
CpG	CpGenerator
CpC	CPCALC+
EP	EnergyPlus
ES	Energy savings (%)
GR	Groningen
IGDG	Italian climatic data collection Gianni De Giorgio
IWEC	International Weather for Energy Calculation
IN	Innsbruck
L	Local
MDM	Mediterranean mountains
MDN	Mediterranean north
MDS	Mediterranean south
MU	Munich
$\hat{q}$	Complex heat flow density (W/m^2)
Q	Energy demand per unit area (kWh/m^2)
$\dot{Q}$	Load per unit area (W/m^2)
PA	Palermo
RO	Rome
T	Temperature (°C)
TPU	Tokyo Polytechnic University
U	Wind speed (m/s)
Y_{mn}	Periodic thermal transmittance (W/(m^2.K))
Y_{nn}	Thermal admittance (W/(m^2.K))

Greek symbols

α	Wind incident angle (°)
$\hat{\theta}$	Complex temperature (°C)

Subscripts

C	Cooling
ceiling	Ceiling
min	Minimum
in	Indoor
N	Night
NV	Night-ventilated
sp	Set point
out	Outdoor
UV	Unventilated

2. Materials and methods

A sensitivity study is first carried out by imposing constant night ventilation rates in the occupied zones of the building to establish a general framework for the analysis of the energy saving potential of night ventilation. Increased Air Change per Hour (ACH) from 0.5 to 20 h^{-1} are imposed during the night (Tab. 1) and the related cooling energy savings (ES) are evaluated by considering the percentage of energy saving in the night-ventilated case (NV) with respect to the unventilated case (UV). The influence of local climate is considered by repeating the analysis for several European locations.

Next, the effects of different sets of C_p on the ventilation rates and on the cooling energy savings (ES) of a night-ventilated office are explored using the AFN model in EnergyPlus. In this case, variable ACH values are derived from the hourly wind conditions in the weather file. Night-averaged ACH and energy savings of the building are calculated over the simulation period (June to August) for different sources of C_p. The sensitivity of the cooling energy savings to the C_p source is tested for different design conditions, simulation parameters, and European climates as listed in Tab. 1.

2.1. Building characteristics

An isolated six-story office building with dimensions 16 m x 24 m x 18 m is modeled with EnergyPlus (Fig. 1a). Each floor is composed of 12 office rooms of 3.4 m x 6.1 m x 2.7 m aligned on the northern and southern sides of the building as shown in Fig. 1b. In each office room daylighting is ensured by non-operable large windows of 2.4 m x 1.2 m on the external walls. To achieve cross-ventilation, operable bottom-hung windows are added on external walls above the others and on internal walls above the doors. The external and internal operable windows sizes are 2.4 m x 0.6 m and 3.4 m x 0.6 m respectively. External shading devices are placed on the large non-operable windows to avoid overheating.

A building structure with high thermal inertia is selected to promote night cooling for the baseline case. An additional case with lower thermal inertia of the exposed thermal mass (BG-1) is defined by moving the insulation layer from the outer to the inner part of the external wall and by adding a suspended ceiling. In order to evaluate the thermal inertia of the structures, dynamic properties are calculated according to the admittance method reported in CEN EN ISO 13786 [36], as in [37, 38]. In particular, the complex quantities periodic thermal transmittance Y_{mn} (m≠n) and internal admittance Y_{nn} are calculated as in Eq. 2:

$$Y_{mn} = -\frac{\hat{q}_m}{\hat{\theta}_n} \tag{2}$$

where $\hat{q}_m$ is the density of heat flow rate through the surface of the component adjacent to zone m and $\hat{\theta}_n$ is the temperature in zone n. Y_{mn} and Y_{nn} express the response of the components to the variation of the outdoor and indoor conditions respectively and their arguments refer to the associated time lag or time lead. Thermal properties of the building structures are thus summarized in Tab. 2. Note that the internal admittance decreases significantly from the baseline case to the case with low thermal inertia.
External glazed surfaces are composed of double pane low-emissivity windows filled with Argon.

2.2 Occupancy and systems

Internal heat gains in the office rooms are defined according to [39] as 20 W/m² in the occupancy period (weekdays, 7 a.m. - 6 p.m.) and as 2 W/m² otherwise. In the corridor internal heat gains of 8 W/m² are scheduled in the occupancy period and 1 W/m² otherwise. A case with high internal heat gains (BG-2) is defined assuming a value of 28 W/m² in the office rooms during the occupancy period according to the range reported in [27].
An ideal air cooling system defined by EnergyPlus (Ideal load HVAC system [30]) is used to determine the cooling energy demand for given set point temperatures (T_{sp}) depending on the climate (26°C for the Italian and 25°C for the other locations). A case with a lower cooling set point temperature (BG-3) is then defined by setting $T_{sp} = 24°C$. The cooling system is active from 8 a.m. to 7 p.m.

2.3 Thermal model

Similar thermal conditions are assumed for each floor of the building. Therefore only the second floor is explicitly modeled in EnergyPlus and adiabatic conditions are selected for the floor and the ceiling surfaces. Each office room and the corridor are modeled as separate thermal zones, as shown in Fig. 1b.
The TARP algorithm [40] is used for simulating natural convection at the internal surfaces. The model correlates the CHTC with surface type, heat flow direction, and temperature difference between indoor air and surfaces [30]. Since both the external and the internal operable openings are located in the upper part of the walls (Fig. 1c) the ventilation flow is expected to impact mainly the convective heat transfer at the ceiling. Thus, a case with an enhanced $CHTC_{ceiling}$ equal to 10 W/ (m².K) during the night is considered (BG-5).

2.4 Climates

Several locations across Europe were selected to test the influence of local climate on the sensitivity of the cooling energy savings to the C_p sources. The locations were chosen in accordance with the study by Metzger et al. [41] that provides a high-resolution climatic stratification of Europe. Within the 13 Environmental Zones in [41], six cities were selected (Tab.3), i.e. Groningen (Atlantic North Zone); Munich (Continental Zone), Innsbruck (Alpine South Zone), Bergamo (Mediterranean Mountains Zone), Rome (Mediterranean North Zone), and Palermo (Mediterranean South Zone).
Meteorological data from the International Weather for Energy Calculation (IWEC) [42] dataset and from the Italian Climatic data collection Gianni De Giorgio (IGDG) [43] are used (Tab.3). All data refer to a Typical Meteorological Year, formed by hourly data from appropriate months of different years as indicated in the local standards [44]. For the selected locations a first indication of the potential for night cooling can be obtained by the values for night-averaged outdoor temperature and wind velocity (see Table 3), the latter assumed to be measured at 10 m height in open terrain .

2.5 Ventilation model

The AFN model of the office building is composed of: external nodes on the building facades, internal nodes in the occupied zones (office rooms and corridor), and airflow elements represented by operable windows. Due to some limitations of the AFN model in predicting wind-induced single sided ventilation [45], only a situation of cross-ventilation is analyzed. The wind pressure acting on the windows is determined by assigning at the external nodes a set of C_p values according to surface orientation and wind incident angle. The C_p values are obtained by experiments, database and empirical correlations as presented in Sect. 3. When closed, the operable windows are considered as 'cracks'. When open, the windows are characterized by a discharge coefficient C_D of 0.6 for the external and 0.78 for

the internal windows [46]. Since, according to [29, 47] an uncertainty of ±0.1 can be assumed for C_D a case (BG-4) was defined where the discharge coefficient of the external openings is taken as $C_D = 0.5$.
The ventilation model works as follows (Fig. 1c): during the night (8 p.m. - 7 a.m.) both external and internal bottom hung windows are open at about 20 and 45 degrees respectively; during the day only the internal windows remain open. Note that to avoid excessive cooling the external windows are closed if the indoor night temperature drops below 18°C.

3 Sources of pressure coefficients

Sets of C_p, either local or surface-averaged, can be obtained from primary and secondary sources and used in AFN models. EnergyPlus uses a secondary source to provide default sets of C_p, i.e. the formula by Swami and Chandra (Sect. 3.1). Other secondary sources in this study are CpGenerator (Sect. 3.2), and CPCALC+ (Sect. 3.3), whereas primary sources are the wind tunnel measurements by Tokyo Polytechnic University (Sect. 3.4).

3.1 EnergyPlus (Formula by Swami and Chandra)

The correlation used by EnergyPlus to estimate the surface-averaged C_p for block-shaped low-rise buildings is the formula by Swami and Chandra [31] (Eq. 3). It is based on a non-linear regression whose variables are the wind incident angle (α) and the building side ratio (G), the latter defined as the natural logarithm of the width of the wall under consideration to the width of the adjacent wall [30]. In the present case the building side ratio is 0.66.

$$C_P = 0.6\ln\left[\begin{array}{l} 1.248 - 0.703\sin\left(\dfrac{\alpha}{2}\right) - 1.175\sin^2(\alpha) + 0.131\sin^3(2\alpha G) + \\[2mm] + 0.769\cos\left(\dfrac{\alpha}{2}\right) + 0.07G^2\sin^2\left(\dfrac{\alpha}{2}\right) + 0.717\cos^2\left(\dfrac{\alpha}{2}\right) \end{array}\right] \tag{3}$$

3.2. CpGenerator

CpGenerator [32] is a web-based program developed by the Dutch research center TNO by fitting wind tunnel data [48, 49] into mathematical expressions. The program provides C_p data for a wide range of isolated and non-isolated block-shaped buildings with flat roof. Local and surface-averaged C_p values can be obtained for both low-rise and high-rise buildings. The wind incident profile is described through the roughness of the terrain that in this study is taken equal to 0.2 m (suburban terrain).

3.3. CPCALC+

CPCALC+ is a program developed within the European Research Program PASCOOL [50, 51] as an upgrade of the code CPCALC [33], implemented at the Lawrence Berkeley Laboratory in California for the COMIS multizone airflow calculation model [22]. A regression analysis was carried out using existing wind tunnel data [52, 53] and new tests performed within the PASCOOL project [54]. The program calculates local and surface-averaged C_p for block-shaped buildings with flat, shed or gable roofs and takes into account the influence of environmental factors, i.e. incident wind profile exponent and presence of surrounding buildings, described in terms of plan area density and building heights. In this study a wind profile exponent of 0.2 (suburban terrain) is considered.

3.4. Wind tunnel tests by Tokyo Polytechnic University (TPU)

An extensive online experimental database of C_p for isolated and non-isolated low-rise buildings is provided by TPU [34,35]. The database consists of wind tunnel data from 111 reduced-scale configurations of rectangular shaped building models for various urban densities. The building models have a fixed plan area of 0.24 m x 0.16 m (scale 1:100) and variable heights of 0.06, 0.12, or 0.18 m. Measurements were performed in the TPU Atmospheric Boundary Layer wind tunnel assuming an inlet profile corresponding to suburban terrain as in the terrain category III of AIJ [55], i.e. with a wind velocity profile exponent of 0.2 and a gradient height of 450 m. C_p values were calculated from the static pressure measured on the surfaces of the central building with pressure taps at every 20 mm. Surface-averaged C_p values for each wind incident angle are provided as well as the local values at the measurement points. In this paper the surface-averaged C_p values (TPU-A) obtained with the wind tunnel test for an isolated building model, which correspond to a real building sized 16 m x 24 m x 18 m (full-scale), were used. Since the measurement points are not matching the opening positions, the local C_p values derived from the measurements are not included in the present analysis.

4. Results and remarks

4.1. Influence of primary and secondary sources on the estimation of C_p values

The influence of C_p sources on surface-averaged C_p values for different wind directions is shown in Fig. 2a, taking as an example the southern facade of the building. With respect to the values from EnergyPlus (EP-A), it is observed that differences up to 45-50% are found with the surface-averaged C_p from CpGenerator (CpG-A) and CPCALC+ (CpC-A) for incidence angles of about 30° and 120° respectively. In Fig. 2b surface-averaged C_p values obtained with CpGenerator (CpG-A) for west wind direction are compared with local values (CpG-L) at window height on different floors (1st, 2nd, and 5th). Significant differences from the surface-averaged values are observed for the windward and the lateral side of the building; in particular, a variation up to 34% is found for the windward side. The impact of these differences on the ventilation rates and on the energy savings of the isolated office building is discussed in the following sections.

4.2. Sensitivity of the cooling energy savings to the variation of constant night ventilation rates

A sensitivity study with constant ventilation rates (ACH_N) varying from 0.5 to 20 h^{-1} is conducted for several European locations listed in Tab. 1 and the results are summarized in Fig. 3.
Clearly for a given value of ACH_N, the lower the night-averaged outdoor temperature reported in Tab. 3, the higher are the energy savings. One further consideration is related to the range of ACH_N giving the largest sensitivity of the energy savings in different climates. In the northern locations of Groningen (GR) and Munich (MU), the night-averaged outdoor temperatures drop below 15 °C. In these cases even small variations of the ACH_N cause a significant impact on the energy savings when ACH_N are less than 5 h^{-1}. Above this threshold the percentage of energy savings is much less related with the ACH_N. A different situation is shown for the southern locations that show a rather low impact of the ACH_N on the energy savings even for values below 5 h^{-1}. In the latter locations substantial differences in the energy savings are expected only for a large variation of the ventilation rates. An extreme case is represented by Palermo (PA), where the night-averaged outdoor temperature is only 2 °C below the cooling set point temperature of 26 °C. Thus, a very low cooling potential is associated with this climate and the dependency of the energy savings to the variation of the ACH_N is extremely low.

4.3 Sensitivity of the cooling energy savings to different C_p sources for Bergamo (BG)

The AFN model predicts variable ventilation rates from the wind conditions listed in the weather file, i.e. hourly wind speed and direction, and the pressure coefficients on the envelope. When ventilation is active, hourly ACH are therefore provided to the thermal analysis in EnergyPlus to calculate the energy demand. An example of the calculation for a south-oriented office room at the 2nd floor in Bergamo (BG) is shown in Fig. 4 for three summer days (July 26-28). Fig. 4a illustrates that during the night both the amount and the sign of the ACH may vary, with positive values meaning that outdoor air comes directly into the room and negative values meaning that air from the corridor comes into the room. During the first night, very little outdoor fresh air is entering the room and the consequent reduction of the minimum indoor air temperature (Fig. 4b) is limited to $T_{in,NV} = 23.5$°C. A very different scenario happens during the second night, where the large amount of air entering the room purges the heat stored in the building structures and the minimum indoor temperature drops to 21.6 °C. As a consequence, the peak in the cooling load on June 27 decreases from $\dot{Q}_{C,UV} = 43.5$ W/m² for the unventilated case to $\dot{Q}_{C,NV} = 36.6$ W/m² for the night-ventilated case (Fig. 4c). Due to the effect of larger ventilation rates, the cooling energy savings increase from 10% on July 26 to 21% on July 27.
Results obtained for the case of Bergamo (BG) over the entire simulation period (June to August) are reported in Fig. 5 considering a single office room and the whole building. It can be observed in Fig. 5a that the choice of the C_p source impacts the estimated ACH_N. Regarding the whole building, differences up to 15% are reported when C_p values are extracted from CPCALC+ (CpC-A) instead of EnergyPlus (EP-A). Also, the use of wind tunnel data (TPU-A) causes differences of almost 10% on the results. Significant variations of ACH_N are also observed for the single room, not only due to the choice of the C_p source, but also due to the use of surface-averaged instead of local C_p. For instance, in the south-oriented room, a variation of 12% in ACH_N is reported (Fig. 5a) when ACH_N are estimated using local C_p from CPCALC+ (CpC-L) instead of the correspondent surface-averaged values (CpC-A). Moreover, a variation of almost 20% is found for the south-west oriented room due to the use of surface-averaged C_p from CPCALC+ (CpC-A). To summarize, the dispersion of the C_p values due to different data sources causes a variation in the predicted ACH_N up to 15% for the whole building and up to about 20% for the single room.
In turn, the impact of the C_p sources is less pronounced when the energy savings are considered. As shown in Fig. 5b, the energy savings over the simulation period for the whole building range from a minimum of 31.3% (CpC-A) to a maximum of about 33.8% (EP-A, CpG-A, CpG-L). With respect to the case with C_p from EnergyPlus (EP-A), a variation up to 2.4% is obtained with C_p values from CPCALC+ (CpC-A). For the single office room, a similar situation is observed.

The difference between the energy savings (ES) of the cases with surface-averaged C_p from CPCALC+ (ES_{CpC}) and from EnergyPlus (ES_{EP}) is referred as to the "sensitivity to C_p source". Its daily variation in June and July is shown in Fig. 6. Overall, it can be noticed that the sensitivity tends to increase with the temperature difference between the indoor set point (T_{sp}) and the outdoor night-averaged ($T_{out,N}$) temperatures.

4.4. Sensitivity of the cooling energy savings to the C_p source: influence of design conditions and simulation parameters

The sensitivity of the energy savings to the C_p source for different design conditions and simulation parameters listed in Tab.1 is evaluated for the case of Bergamo (BG). Fig. 7a and 7b and Tab. 4 report the results achieved for the baseline case (BG) and for the cases obtained by varying some design conditions, i.e. thermal inertia of the exposed thermal mass (BG-1), internal heat gains (BG-2) and set point temperature (BG-3), and simulation parameters, i.e. discharge coefficient of the external openings (BG-4) and CHTC of the ceiling (BG-5). Note that the case with C_p from EnergyPlus (EP-A) is the reference for calculating the variation of ACH_N with C_p and the sensitivity of ES to C_p in Tab.4.

Fig. 7a and 7b compare the influence of the above mentioned cases on the $ACH_{N,EP}$ and the ES_{EP} obtained using the C_p from EnergyPlus (EP-A). The error bars in Fig. 7a and 7b indicate the maximum variations due to the source of C_p. As expected, the night-ventilation rates (ACH_N) are only affected by the variation of the discharge coefficient of the external openings (case BG-4), as shown in Fig. 7a. As regards to the Energy Savings (ES), it can be observed (Fig.7b) that ES for the baseline case (BG) lower from 33.7% to 32.0% when the exposed thermal mass has a lower thermal inertia (case BG-1), since the heat stored in the thermal mass is reduced. Similarly, ES of the baseline case are reduced for both the cases with higher internal heat gains (BG-2) and with lower set point temperature (BG-3). This is due to the fact that the cooling energy demand of the unventilated buildings $Q_{C,UV}$ (Tab. 4) increases with respect to the baseline case. Finally, as the C_D of the external openings is reduced (BG-4), the night-ventilation rates (ACH_N) are lower and the ES decrease to 30.1%. In turn, when increasing the $CHTC_{ceiling}$ (BG-5) the ES increase to 37.0% because of the enhanced heat transfer between the fresh air and the thermal mass.

However it is observed that in all cases considered the sensitivity of ES to the C_p source has not significantly varied with respect to the baseline case (Tab. 4 and Fig. 7b) and ranges between a minimum of 1.9% (BG-3) and a maximum of 2.7% (BG-5). Therefore only the baseline case is used for further analysis.

4.5. Sensitivity of the cooling energy savings to the C_p source: influence of the meteorological conditions

An overview of the results obtained by repeating the sensitivity analysis to the C_p source of the baseline case for different European locations (Tab. 1) is given in Tab. 5.

Night-averaged ACH vary from a minimum of 2.2 h^{-1} in Bergamo (BG) and 2.5 h^{-1} in Innsbruck (IN) to a maximum of 4.8 h^{-1} in Groningen (GR) and 5.2 h^{-1} in Palermo (PA). However, for all cases, a maximum sensitivity of almost 17% is reported for the use of C_p values from CPCALC+ (CpC-A), as for Bergamo (BG).

Similar to the results in Sect. 4.3 and Sect. 4.4, much lower sensitivity to the C_p sources is obtained when considering the energy savings, with higher values related to the use of surface-averaged C_p from CPCALC+ (CpC-A). To this extent, maximum sensitivity of about 4% is found in Groningen (GR), followed by the 3.3% in Munich (MU).

A comparison between these results and the ones achieved by imposing constant night ventilation rate is presented in Fig. 8, where energy savings obtained with AFN model analysis (Tab. 5) are superimposed to the corresponding curves from the sensitivity analysis (Fig. 3). Although the results do not match perfectly, the sensitivity of the energy savings to the C_p sources is consistent with the sensitivity of the energy savings to the ACH_N. The differences are due to the fact that in the AFN model analysis ACH_N is obtained as an average of variable flow rates, both in terms of quantity and in terms of flow direction.

4.6 Limitations of the study

The study focuses on a simplified and widely investigated building geometry for which many different primary and secondary C_p sources are available. Contrary to what might be expected the variety of C_p data has only a minor impact on the predicted energy savings for night ventilation. This is also reported by previous studies (e.g. [29]) that mainly focused on the sensitivity of indoor thermal comfort conditions to the dispersion of the C_p data related with uncertainties in the wind shielding conditions. Breesch and Janssens [29] found that other input parameters such as the internal heat gains or the air tightness are more dominant for the evaluation of thermal comfort in naturally night ventilated buildings.

In the case under study, the low sensitivity of the cooling energy savings to the C_p source might be due to the fact that the C_p values extracted from different sources for the case under study show fairly similar values, as can be seen from the overall agreement of the data in Fig. 2a. Nevertheless, the results are of general interest, since they show that in some circumstances the choice of the C_p source is not critical for the prediction of the natural ventilation effects. Further work should address the impact of the C_p sources on night cooling for more complex building geometries.

5. Conclusions

In the present study the influence of primary and secondary sources of pressure coefficients on the evaluation of night ventilation rates and consequent cooling energy savings is assessed. A case study regarding a night-ventilated office building was simulated with EnergyPlus and the embedded AFN model for different design conditions and simulation parameters. Furthermore, several European climates were considered to cover a wide range of wind and temperature conditions.

The analysis of the surface-averaged C_p from different sources points out local differences for certain wind directions in spite of an overall agreement. This might be due to the choice of a simple geometry such as an isolated block-shaped low-rise building. For this geometry, several C_p sources are available, giving the opportunity to show a detailed analysis method. On the other hand, limited differences among the C_p from the selected sources are also impacting the final results.

When considering the predicted night ventilation rates, different C_p sources have significant influence. Differences up to 15% are reported on the night-averaged ACH for the whole building and up to almost the 20% for a single room. With regard to energy savings, an analysis conducted with increased constant ACH_N shows that the sensitivity of the cooling energy savings to the ACH_N tends to be higher in those climates where larger differences are found between the night-averaged outdoor air temperature and the indoor set point temperature. This result is confirmed by the analysis conducted with the AFN model. For the current case, however the energy savings due to wind-driven night ventilation are only marginally influenced by the dispersion of the C_p from different sources. Since in the present study some key parameters influencing the building cooling demand (internal gains, set point temperature) and the ventilation effectiveness (thermal mass, internal convective heat transfer coefficients, discharge coefficients of the openings) were varied, it can be stated that this outcome holds for a wide range of design and simulation parameters. The present study extends thus the results achieved by Breesch and Janssens [29], by considering the dispersion of C_p data caused by the different sources and by analyzing the cases in which natural night ventilation is used to reduce the daily cooling demand of office buildings.

The results of the present study lead to the useful conclusion that the choice of a given C_p source strongly affects the accuracy of the predicted airflow rates for natural ventilation, but it is not critical when predicting the passive cooling effects of night ventilation for an isolated block-shaped low-rise building.

References

[1] European Directive 2002/91/CE. Directive 2002/91/EC of the European Parliament and of the Council of 16 December 2002 on the energy performance of buildings:2002.

[2] CIBSE TM. Climate change and the indoor environment: impacts and adaptation.Chartered Institute of Building Services Engineers, London 2005.

[3] Yang L, Li Y. Cooling load reduction by using thermal mass and night ventilation. Energy Build 2008;40:2052-8.

[4] Balaras CA. The role of thermal mass on the cooling load of buildings. An overview of computational methods. Energy Build 1996;24:1-10.

[5] Blondeau P, Spérandio M, Allard F. Night ventilation for building cooling in summer. Sol Energy 1997;61:327-35.

[6] Shaviv E, Yezioro A, Capeluto IG. Thermal mass and night ventilation as passive cooling design strategy. Renew Energ 2001;24:445-52.

[7] Givoni B. Comfort, climate analysis and building design guidelines. Energy Build 1992;18:11-23.

[8] Geros V, Santamouris M, Karatasou S, Tsangrassoulis A, Papanikolaou N. On the cooling potential of night ventilation techniques in the urban environment. Energy Build 2005;37:243-57.

[9] Artmann N, Manz H, Heiselberg P. Climatic potential for passive cooling of buildings by night-time ventilation in Europe. Appl Energy 2007;84:187-201.

[10] Ramponi R, Blocken B. CFD simulation of cross-ventilation flow for different isolated building configurations: validation with wind tunnel measurements and analysis of physical and numerical diffusion effects. J Wind Eng Ind Aerodyn 2012;104:408-18.

[11] Ramponi R, Blocken B. CFD simulation of cross-ventilation for a generic isolated building: Impact of computational parameters. Build Environ 2012;53:34-48.

[12] Chen Q. Ventilation performance prediction for buildings: A method overview and recent applications. Build Environ 2009;44:848-58.

[13] Franke J, Hellsten A, Schlünzen H, Carissimo B. Best practice guideline for the CFD simulation of flows in the urban environment. 2007.

[14] Tominaga Y, Mochida A, Yoshie R, Kataoka H, Nozu T, Yoshikawa M et al. AIJ guidelines for practical applications of CFD to pedestrian wind environment around buildings. J Wind Eng Ind Aerodyn 2008;96:1749-61.

[15] van Hooff T, Blocken B. Coupled urban wind flow and indoor natural ventilation modelling on a high-resolution grid: A case study for the Amsterdam ArenA stadium. Environ Modell Softw 2010;25:51-65.

[16] Karava P, Stathopoulos T, Athienitis AK. Airflow assessment in cross-ventilated buildings with operable façade elements. Build Environ 2011;46:266-79. [17] Gu L. Airflow Network Modeling in EnergyPlus. In: Proceedings of Building Simulation 2007:964-71.

[18] Hensen JLM, Lamberts R. Building Performance Simulation for Design and Operation. London: Routledge, 2011.

[19] Axley J. Multizone airflow modeling in buildings: History and theory. HVAC&R Res 2007;13:907-28.

[20] Costola D, Blocken B, Ohba M, Hensen J. Uncertainty in airflow rate calculations due to the use of surface-averaged pressure coefficients. Energy Build 2010;42:881-8.

[21] Costola D, Blocken B, Hensen JLM. Overview of pressure coefficient data in building energy simulation and airflow network programs. Build Environ 2009;44:2027-36.

[22] Feustel HE, Rayner-Hooson A. COMIS fundamentals. Report LBL-28560, US Department of Energy, Lawrence Berkeley Laboratory 1990.

[23] Swami MV, Chandra S. Procedures for calculating natural ventilation airflow rates in buildings. ASHRAE Final Report FSEC-CR-163-86, ASHRAE Research Project 1987.

[24] Artmann N, Manz H, Heiselberg P. Parameter study on performance of building cooling by night-time ventilation. Renew Energ 2008;33:2589-98.

[25] Ascione F., Bianco N., De Masi R.F., de Rossi F., Vanoli G.P. Energy refurbishment of existing buildings through the use of phase change materials: Energy savings and indoor comfort in the cooling season. Appl Energy 2014; 113, 990-1007.

[26] Eicker U. Cooling strategies, summer comfort and energy performance of a rehabilitated passive standard office building. Appl. Energy 2010; 2013-2039.

[27] Goethals K, Breesch H, Janssens A. Sensitivity analysis of predicted night cooling performance to internal convective heat transfer modelling. Energy Build 2011;43:2429-41.

[28] Kolokotroni M, Aronis A. Cooling-energy reduction in air-conditioned offices by using night ventilation. Appl Energy 1999;63:241-53.

[29] Breesch H, Janssens A. Performance evaluation of passive cooling in office buildings based on uncertainty and sensitivity analysis. Sol Energy 2010;84:1453-1467.

[30] DOE U. EnergyPlus Engineering reference. 2010.

[31] Swami M, Chandra S. Correlations for pressure distribution on buildings and calculation of natural-ventilation airflow. ASHRAE Trans 1988;94:243-66.

[32] Knoll B, Phaff J, de Gids W. Pressure coefficient simulation program. AIR 1996;17:1-5.

[33] Grosso M. Wind pressure distribution around buildings: a parametrical model. Energy Build 1992;18:101-31.

[34] Quan Y, Tamura Y, Matsui M, Cao S, Yoshida A, Xu S. Interference effect of a surrounding building group on wind loads on flat roof of low-rise building: Part I, Distribution of local wind pressure coefficient. Wind Engineers, JAWE 2007;32:211-2.

[35] Quan Y, Tamura Y, Matsui M, Cao S, Yoshida A, Xu S. Interference effect of a surrounding building group on wind loads on flat roof of low-rise building: Part II, Interference factor of worst extreme local and area-averaged suction pressure coefficients. Wind Engineers, JAWE 2007;32:213-4.

[36] CEN. EN ISO 13786:2007, Thermal performance of building components—dynamic thermal characteristics - calculation method. 2007.

[37] Aste N, Angelotti A, Buzzetti M. The influence of the external walls thermal inertia on the energy performance of well insulated buildings. Energy Build 2009;41:1181-7.

[38] Rossi M, Rocco VM. External Walls Design: The Role Of Periodic Thermal Transmittance And Internal Areal Heat Capacity. Energy Build 2012.

[39] UNI/TS 11300-1: 2008: Energy performance of buildings Part 1: Evaluation of energy need for space heating and cooling. 2008.

[40] Walton GN. Thermal analysis research program reference manual. 1983;NBSIR 83-2655.

[41] Metzger M, Bunce R, Jongman R, Mücher C, Watkins J. A climatic stratification of the environment of Europe. Global Ecol Biogeogr 2005;14:549-63.

[42] ASHRAE. International Weather for Energy Calculations (IWEC Weather Files) Users Manual and CD-ROM. 2001.

[43] Mazzarella L. Dati climatici G. De Giorgio. Proceedings of giornata di studio Giovanni De Giorgio, Politecnico di Milano, Milano 1997.

[44] CEN. EN ISO 15927-4: 2005, Hygrothermal performance of buildings – calculation and presentation of climatic data. Part 4: data for assessing the annual energy for heating and cooling. 2005.

[45] Johnson M., Zhai Z.J., Krarti M. Performance evaluation of network airflow models for natural ventilation. HVAC&R Research 2012;18:3:349-365.

[46] Santamouris M, Asimakopoulos D. Passive cooling of buildings. : Earthscan/James & James, 1996.

[47] Flourenztou F., Van der Maas J., Roulet C.A. Natural ventilation for passive cooling: measurement of discharge coefficients. Energy Build 1998; 27:3:283-292.

[48] Phaff J. Continuation of model tests of the wind pressure distribution on some common building shapes. TNO report 1979;C429 (in Dutch).

[49] Phaff J. Model tests of the wind pressure distribution on some common building shapes. TNO report 1977;C403 (in Dutch).

[50] Grosso M. Modelling wind pressure distribution on buildings for passive cooling. In: Proceedings of the International conference solar energy in architecture and urban planning. Commission of the European Communities, May 17-21, Florence, Italy; 1993:17-21.

[51] Grosso M, Mariano D, Parisi E. Wind pressure distribution on flat and tilted roofs: a parametrical model. In: Proceedings of the European conference on energy performance and indoor climate in buildings, November 24-26, Lyon, France; 1994:167-172.

[52] Akins R, Cermak J. Wind pressures on buildings, Fluid dynamics and Diffusion Laboratory. Report CER76-77REAJEC15, Colorado State University, Fort Collins 1976.

[53] Hussein M, Lee B. An investigation of wind forces on three dimensional roughness elements in a simulated atmospheric boundary layer. BS55, University of Sheffield, UK 1980.

[54] Marques da Silva F, Saraiva JG. Determination of pressure coefficients over simple shaped building models under different boundary layers, Minutes of the PASCOOL-CLI meetings, Florence, May 1993, Segovia, November 1993, WInd tunnel reports, Lisbon, January, March, 1994. 1994.

[55] Architectural Institute of Japan (AIJ). Recommendations for loads on buildings. 2004.
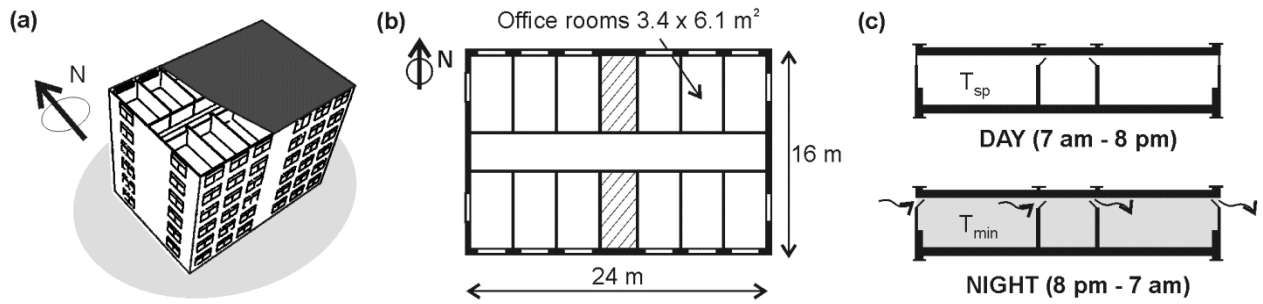
FIGURE CAPTIONS

Figure 1. (a) Building geometry and (b) plan of a typical floor with 12 office rooms sized 3.4 x 6.1 m² (in white the occupied zones), and (c) schedules of the natural ventilation system. During the day, windows are closed and the cooling set point temperature (T_{sp}) is 26°C for the Italian locations and 25°C otherwise. During the night, the ventilation is active and a minimum indoor temperature (T_{min}) of 18°C is imposed to avoid excessive cooling.
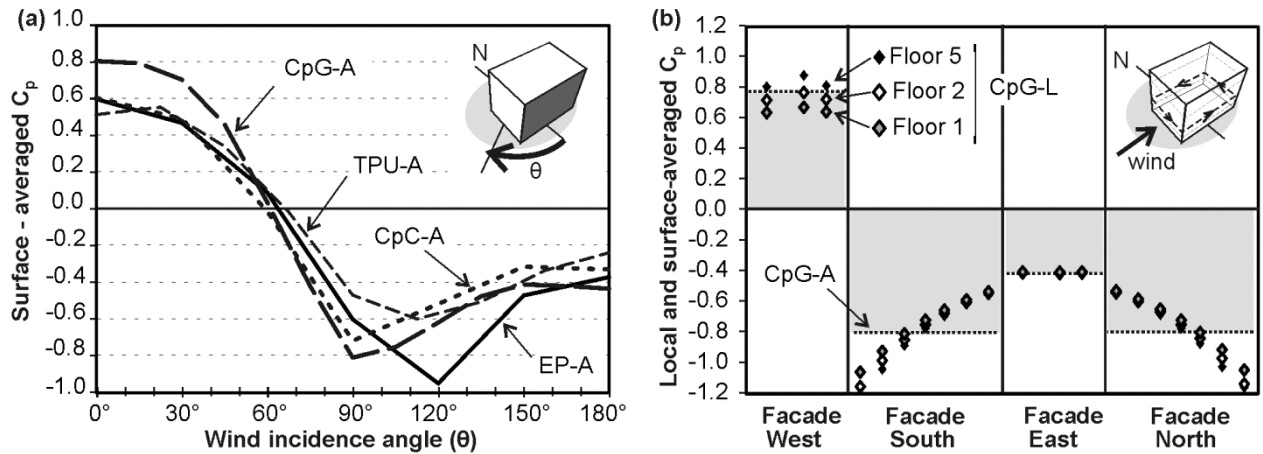

Figure 2. (a) Surface-averaged C_p on the southern facade of the building versus wind incidence angles (θ) for different C_p sources, i.e. EnergyPlus (EP-A), CpGenerator (CpG-A), CPCALC+ (CpC-A), and wind tunnel tests (TPU-A); (b) Local C_p at window height on the 1st, 2nd and 5th floors obtained with CpGenerator (CpG-L) for west wind direction and comparison with the surface-averaged C_p obtained with the same source (CpG-A).
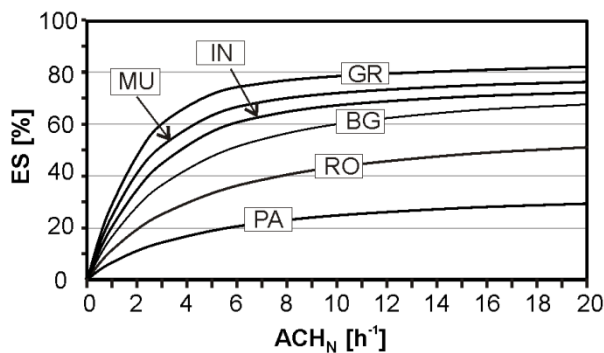

Figure 3. Effects of the increased constant night ventilation rate (ACH_N) on the energy savings (ES) of the building in different European climates (Tab. 3).
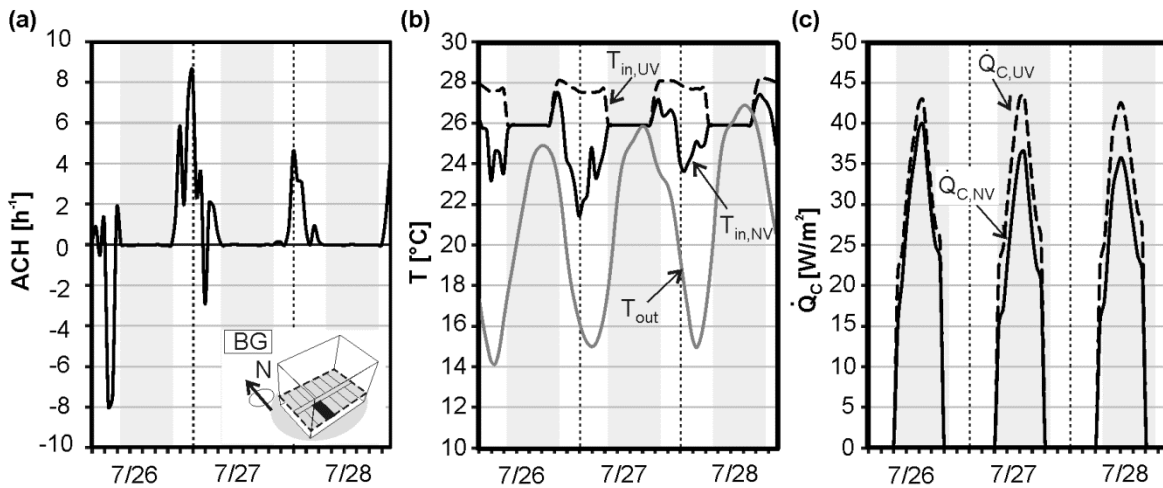
Figure 4. (a) ACH in a south-oriented office room during three summer days (July 26-28) in Bergamo (BG); (b) Outdoor temperature (T_{out}) and indoor temperature in the night ventilated ($T_{in,V}$) and unventilated ($T_{in,UV}$) cases; (c) Cooling load per unit area of the night ventilated ($\dot{Q}_{C,NV}$) and unventilated ($\dot{Q}_{C,UV}$) cases.

Figure 5. Effect of the C_p sources (a) on the night-averaged ACH (ACH_N) and (b) on the energy savings (ES) estimated over the simulation period for a south-oriented office room and for the whole building in Bergamo (BG). C_p are extracted from EnergyPlus (EP-A), CpGenerator (CpG-A, CpG-L), CPCALC+ (CpC-A, CpC-L), and TPU database (TPU-A).

Figure 6. Impact of the temperature difference between the indoor set point temperature (T_{sp}) and the night-averaged outdoor temperature ($T_{out,N}$) on the sensitivity of ES to the C_p for the months of June and July in Bergamo (BG). The sensitivity of the ES to C_p is the difference between the daily energy savings of the case with surface-averaged C_p from EnergyPlus (ES_{EP}) and from CPCALC+ (ES_{CpC}).

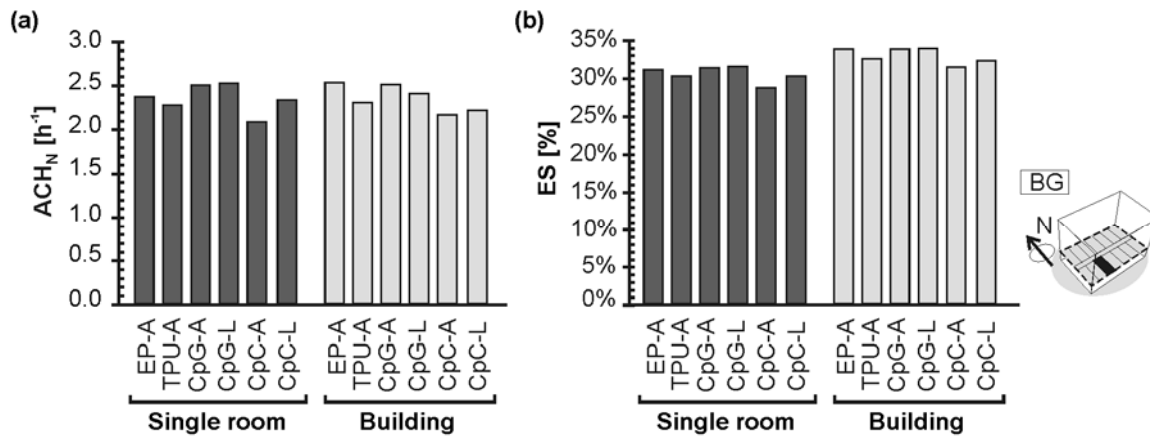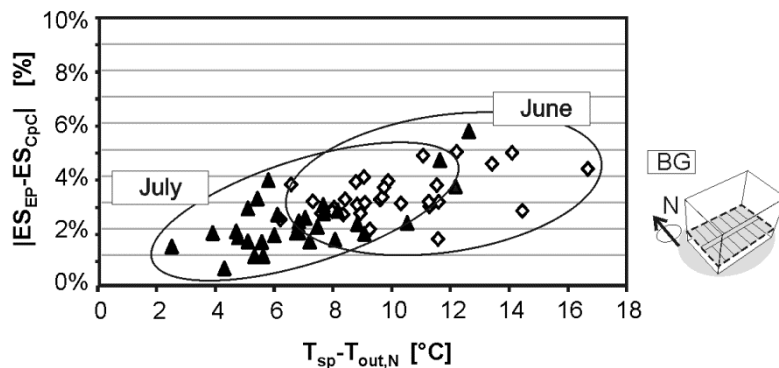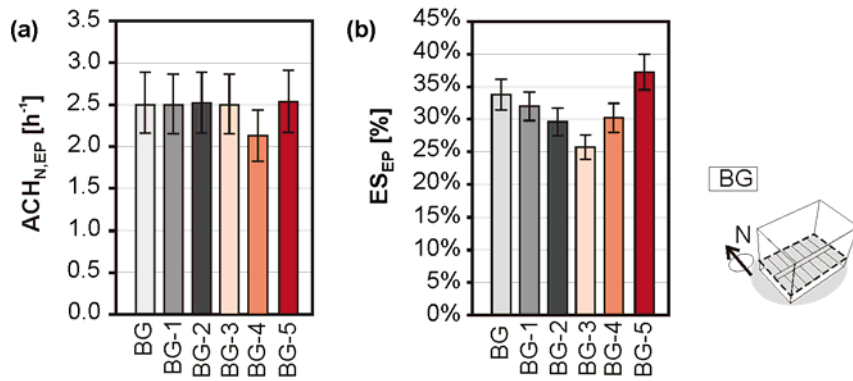Figure 7. Effect of different design conditions and simulation parameters (a) on the night-averaged ACH (ACH_N) and (b) on the energy savings (ES) estimated over the simulation period for the whole building in Bergamo (BG) using the C_p from EnergyPlus (EP-A). The error bars represent the maximum variation due to the C_p source, as reported in Tab. 4. The cases analyzed are: the baseline (BG); the low thermal inertia of the exposed thermal mass (BG-1); the high internal heat gains in the office rooms (BG-2); the lower set point temperature (BG-3); the lower discharge coefficient of the external openings (BG-4); and the enhanced $CHTC_{ceiling}$ (BG-5).
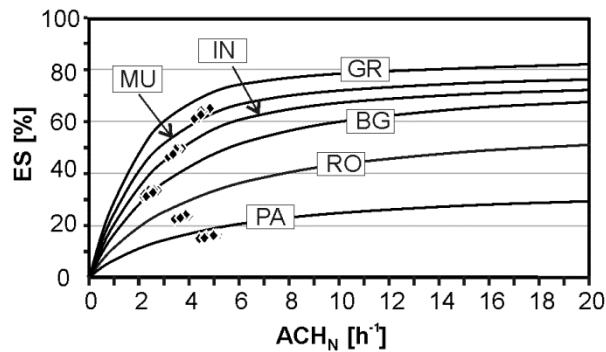
Figure 8. Energy savings (ES) versus night ventilation rates (ACH_N). Comparison between the results obtained from the constant ventilation rate analysis (lines) and the AFN model analysis (dots) for different European locations over the whole simulation period (June to August).

Table 1. Summary of the cases under study: case location and features and night ventilation parameters for the unventilated (UV) and the night-ventilated (NV) cases tested with (i) constant night ventilation rates (ACH_N) and (ii) AFN model (C_p sources).

| Case	Location	Case features	(i) Constant ventilation rates ACH_N [h^{-1}]		(ii) AFN model C_p sources	
			UV	NV	UV	NV
BG	Bergamo	Baseline case	0.02	0.5-20	EP	EP, CpG, CpC, TPU
GR	Groningen	-	0.02	0.5-20	EP	EP, CpG, CpC, TPU
MU	Munich	-	0.02	0.5-20	EP	EP, CpG, CpC, TPU
IN	Innsbruck	-	0.02	0.5-20	EP	EP, CpG, CpC, TPU
RO	Rome	-	0.02	0.5-20	EP	EP, CpG, CpC, TPU
PA	Palermo	-	0.02	0.5-20	EP	EP, CpG, CpC, TPU
BG-1	Bergamo	Low thermal inertia of the exposed thermal mass	-	-	EP	EP, CpG, CpC, TPU
BG-2	Bergamo	Internal heat gains of the office rooms (28 W/m²)	-	-	EP	EP, CpG, CpC, TPU
BG-3	Bergamo	Set point temperature ($T_{sp} = 24°C$)	-	-	EP	EP, CpG, CpC, TPU
BG-4	Bergamo	Discharge coefficient of the external openings ($C_D = 0.5$)	-	-	EP	EP, CpG, CpC, TPU
BG-5	Bergamo	CHTC of the ceiling ($CHTC_{ceiling} = 10$ W/(m²K))	-	-	EP	EP, CpG, CpC, TPU

Table 2. Thermal properties of the building structure: baseline case and case with lower thermal inertia of the exposed thermal mass (the main differences among the two cases are underlined).

Wall	Composition (inside to outside)	U-value [W/(m²K)]	Periodic Thermal Transmittance (Y_mn)		Internal Admittance (Y_nn)	
			Amplitude [W/(m²K)]	Time lag [h]	Amplitude [W/(m²K)]	Time lead [h]
Baseline case						
External wall	2 cm plaster, 24 cm brick masonry, 8.5 cm polystyrene, 2 cm plaster	0.34	0.04	-11.04	3.96	1.27
Ceiling	1.2 cm cement building board, 15 cm cast concrete, 5 cm screed, 1 cm carpet/underlay	2.04	-	-	5.17	1.11
Floor	1 cm carpet/underlay, 5 cm screed, 15 cm cast concrete, 1.2 cm cement building board	2.04	-	-	4.25	1.19
Partitions	1.3 cm plaster, 16 cm brick masonry, 1.3 cm plaster	1.45	-	-	3.51	1.17
Case with lower thermal inertia of the exposed thermal mass (BG-1)						
External wall	2 cm plaster, 8.5 m polystyrene, 24 cm brick masonry, 2 cm plaster	0.34	0.05	-10.98	1.82	4.19
Ceiling	2 cm suspended ceiling, 25 cm air gap, 1.2 cm cement building board, 15 cm cast concrete, 5 cm screed, 1 cm carpet/underlay	1.34	-	-	2.45	1.18
Floor	1 cm carpet/underlay, 5 cm screed, 15 cm cast concrete, 1.2 cm cement building board, 25 cm air gap, 2 cm suspended ceiling	1.34	-	-	4.28	1.15
Partitions	1.3 cm plaster, 16 cm brick masonry, 1.3 cm plaster	1.45	-	-	3.51	1.17

Table 3: Selected European locations: environmental zones according to [41], meteorological data source and characteristics, i.e. night-averaged outdoor temperature ($T_{out,N}$) and night-averaged wind speed (U_N) during the simulation period (June to August).

Location	Environmental zones	Meteorological data source	Meteorological parameters		
			$T_{out,N}$ [°C]	U_N [m/s]	
Bergamo (BG)	MDM	IGDG	17.9	1.5	
Groningen (GR)	ATN	IWEC	13.1	2.8	
Munich (MU)	CON	IWEC	13.8	2.0	
Innsbruck (IN)	ALS	IWEC	15.1	1.5	
Rome (RO)	MDN	IWEC	20.6	1.7	
Palermo (PA)	MDS	IWEC	23.9	2.2	

Table 4. Results of the AFN model analysis conducted with different design conditions and simulation parameters (Tab. 1) for Bergamo (BG) over the simulation period (June to August): (i) night-averaged ACH (ACH_N) and variation with C_p, calculated with respect to the EP-A case; (ii) total energy demand (Q_C) and savings (ES) due to night ventilation over the simulation period, and sensitivity of ES to C_p. The latter is calculated as $|ES_X-ES_{EP}|$, with X referring to any C_p source and EP to EnergyPlus (EP-A).

Case	C_p source	(i) Night-averaged ACH		(ii) Energy demand and savings		
		ACH_N	Variation of ACH_N with C_p	Energy demand ($Q_{C,NV}$)	Energy savings (ES)	Sensitivity of ES to C_p
		[h^{-1}]	[%]	[kWh/m²]	[%]	[%]
BG: Baseline case ($Q_{C,UV}$ = 26.6 kWh/m²)						
	EP-A	2.5	-	17.6	33.7%	-
	TPU-A	2.3	9.1%	18.0	32.4%	1.3%
	CpG-A	2.5	0.8%	17.6	33.7%	0.0%
	CpG-L	2.4	4.9%	17.6	33.8%	0.1%
	CpC-A	2.2	14.4%	18.3	31.3%	2.4%
	CpC-L	2.2	12.6%	18.1	32.1%	1.6%
BG-1: Thermal inertia of the exposed thermal mass ($Q_{C,UV}$ = 26.7 kWh/m²)						
	EP-A	2.5	-	18.2	32.0%	-
	TPU-A	2.3	8.9%	18.5	30.7%	1.2%
	CpG-A	2.5	0.9%	18.2	31.9%	0.0%
	CpG-L	2.4	4.9%	18.2	32.0%	0.0%
	CpC-A	2.2	14.3%	18.8	29.8%	2.2%
	CpC-L	2.2	12.5%	18.6	30.5%	1.4%
BG-2: Internal heat gains ($Q_{C,UV}$ = 31.0 kWh/m²)						
	EP-A	2.5	-	21.9	29.5%	-
	TPU-A	2.3	9.0%	22.2	28.4%	1.2%
	CpG-A	2.5	0.7%	21.9	29.5%	0.0%
	CpG-L	2.4	4.9%	21.9	29.6%	0.1%
	CpC-A	2.2	14.5%	22.5	27.4%	2.1%
	CpC-L	2.2	12.5%	22.3	28.2%	1.4%
BG-3: Set point temperature ($Q_{C,UV}$ = 28.9 kWh/m²)						
	EP-A	2.5	-	21.5	25.7%	-
	TPU-A	2.3	9.0%	21.8	24.7%	1.0%
	CpG-A	2.5	1.1%	21.5	25.7%	0.0%
	CpG-L	2.4	5.1%	21.5	25.7%	0.0%
	CpC-A	2.2	14.3%	22.0	23.8%	1.9%
	CpC-L	2.2	12.4%	27.6	15.2%	0.9%
BG-4: Discharge coefficient of the external openings ($Q_{C,UV}$ = 26.6 kWh/m²)						
	EP-A	2.1	-	18.6	30.1%	-
	TPU-A	1.9	9.2%	18.9	28.8%	1.2%
	CpG-A	2.1	0.6%	18.6	30.1%	0.1%
	CpG-L	2.0	4.9%	18.6	30.2%	0.1%
	CpC-A	1.8	14.6%	19.2	27.8%	2.2%
	CpC-L	1.9	12.7%	19.0	28.6%	1.5%
BG-5: CHTC of the ceiling ($Q_{C,UV}$ = 26.6 kWh/m²)						
	EP-A	2.5	-	16.8	37.0%	-
	TPU-A	2.3	9.2%	17.2	35.5%	1.5%
	CpG-A	2.5	0.6%	16.7	37.2%	0.1%
	CpG-L	2.4	4.8%	16.7	37.2%	0.2%
	CpC-A	2.2	14.6%	17.5	34.3%	2.7%
	CpC-L	2.2	12.7%	17.2	35.2%	1.8%

Table 5. Results of the AFN model analysis conducted for different European locations (Tab. 1) over the simulation period (June to August): (i) night-averaged ACH (ACH_N) and variation with C_p, calculated with respect to the EP-A case; (ii) total energy demand (Q_C) and savings (ES) due to night ventilation over the simulation period, and sensitivity of ES to C_p. The latter is calculated as $|ES_X-ES_{EP}|$, with X referring to any C_p source and EP to EnergyPlus (EP-A).

Case	C_p source	(i) Night-averaged ACH		(ii) Energy demand and savings		
		ACH_N	Variation of ACH_N with C_p	Energy demand ($Q_{C,NV}$)	Energy savings (ES)	Sensitivity of ES to C_p
		[h^{-1}]	[%]	[kWh/m²]	[%]	[%]
Bergamo (BG): T_{sp} = 26°C; T_{sp} - $T_{out,N}$ = 7.8°C; $Q_{C,UV}$ = 26.6 kWh/m²						
	EP-A	2.5	-	17.6	33.7%	-
	TPU-A	2.3	9.1%	18.0	32.4%	1.3%
	CpG-A	2.5	0.8%	17.6	33.7%	0.0%
	CpG-L	2.4	4.9%	17.6	33.8%	0.1%
	CpC-A	2.2	14.4%	18.3	31.3%	2.4%
	CpC-L	2.2	12.6%	18.1	32.1%	1.6%
Groningen (GR): T_{sp} = 25°C; T_{sp} - $T_{out,N}$ = 12.8°C, $Q_{C,UV}$ = 19.2 kWh/m²						
	EP-A	4.8	-	6.7	65.3%	-
	TPU-A	4.5	7.9%	7.1	63.2%	2.1%
	CpG-A	4.6	5.4%	6.9	64.1%	1.1%
	CpG-L	4.5	7.3%	6.8	64.4%	0.8%
	CpC-A	4.2	12.9%	7.4	61.3%	4.0%
	CpC-L	4.5	7.5%	7.1	62.9%	2.4%
Munich (MU): T_{sp} = 25°C; T_{sp} - $T_{out,N}$ = 12.2°C, $Q_{C,UV}$ = 21.4 kWh/m²						
	EP-A	3.7	-	10.7	49.8%	-
	TPU-A	3.4	8.7%	11.1	48.1%	1.7%
	CpG-A	3.6	4.4%	10.8	49.6%	0.2%
	CpG-L	3.5	7.1%	10.8	49.6%	0.2%
	CpC-A	3.2	14.7%	11.4	46.5%	3.3%
	CpC-L	3.4	9.8%	11.2	47.7%	2.2%
Innsbruck (IN): T_{sp} = 25°C; T_{sp} - $T_{out,N}$ = 10.7°C, $Q_{C,UV}$ = 23.3 kWh/m²						
	EP-A	2.8	-	15.5	33.6%	-
	TPU-A	2.5	10.7%	15.9	32.1%	1.6%
	CpG-A	2.6	5.0%	15.5	33.5%	0.1%
	CpG-L	2.6	5.9%	15.4	33.8%	0.2%
	CpC-A	2.3	16.9%	16.0	31.3%	2.3%
	CpC-L	2.6	6.9%	15.7	32.8%	0.8%
Rome (RO): T_{sp} = 26°C; T_{sp} - $T_{out,N}$ = 4.3°C, $Q_{C,UV}$ = 30.0 kWh/m²						
	EP-A	4.0	-	22.8	23.8%	-
	TPU-A	3.6	9.5%	23.1	22.9%	0.9%
	CpG-A	3.9	2.2%	22.7	24.1%	0.3%
	CpG-L	3.9	3.4%	22.7	24.2%	0.4%
	CpC-A	3.4	14.3%	23.2	22.4%	1.4%
	CpC-L	3.7	8.9%	23.1	22.9%	0.9%
Palermo (PA): T_{sp} = 26°C; T_{sp} - $T_{out,N}$ = 1.0°C, $Q_{C,UV}$ = 32.6 kWh/m²						
	EP-A	5.2	-	27.3	16.1%	-
	TPU-A	4.7	9.2%	27.5	15.5%	0.6%
	CpG-A	5.1	2.0%	27.3	16.2%	0.1%
	CpG-L	5.0	3.8%	27.3	16.2%	0.1%
	CpC-A	4.4	14.8%	27.7	14.9%	1.2%
	CpC-L	4.6	10.9%	27.6	15.2%	0.9%